

HYDRAULIC DESIGN OF FISH-FRIENDLY COST-EFFECTIVE BOX CULVERTS: USING HYBRID MODELLING FOR BETTER DESIGN GUIDELINES

XINQIAN LENG⁽¹⁾ & HUBERT CHANSON⁽²⁾

^(1,2) The University of Queensland, School of Civil Engineering, Brisbane QLD 4072, Australia
e-mail h.chanson@uq.edu.au

ABSTRACT

While important for delivering a range of important socio-economic services, road crossings and culverts are known to block the upstream fish passage, particularly for small-body-mass fish species. Using a combination of physical and numerical CFD modelling, design guidelines were developed for smooth box culverts without appurtenance, with a novel approach based upon the basic concepts: (a) the culvert design is optimised for fish passage for small to medium water discharges, and for flood capacity for larger discharges, and (b) low-velocity zones are provided along the wetted perimeter in the culvert barrel, and quantified in terms of a fraction of the wetted flow area where the local longitudinal velocity is less than a characteristic fish speed linked to swimming performances of targeted fish species. The approach relies upon an accurate physically-based knowledge of the entire velocity field in the culvert barrel, specifically the longitudinal velocity map, given that behavioural observations confirmed that fish prefer to swim upstream in low-velocity zones (LVZs) next to the walls and bottom corners. While the focus of the study is on the upstream passage of small-body-mass fish, typical of Australian native fish species, the approach and methodology are relevant to most box culvert structures.

Keywords: Standard box culverts, Upstream fish passage, Hydraulic engineering, Small-body-mass fish, Low-velocity zones.

1 INTRODUCTION

River crossings and culverts are important for delivering a range of socio-economic services, including transportation and hydrological control. These structures are also known to have negative impacts on freshwater river system morphology and ecology, including the blockage of upstream fish passage, particularly small-body-mass fish species (Warren and Perdey 1998, Anderson et al. 2012, Wang and Chanson 2018a). Freshwater fish species constitute about one quarter of all living vertebrates, and are considered an at-risk group due to deleterious habitat impacts. In Australia, for example, there are about 250 freshwater fish species, with approximately 30% listed as threatened under State and Commonwealth legislations (Allen et al. 2002, Lintermans 2013). The negative effects of river crossings on freshwater fish species have been well documented in the literature (Briggs and Galarowicz 2013). Culvert structures create physical or hydrodynamic barriers that often prevent or reduce access to essential breeding and feeding habitats. Common culvert fish passage barriers include excessive vertical drop at the culvert outlet (perched outlet), high velocity or inadequate flow depth within the culvert barrel, excessive turbulence, and debris accumulation at the culvert inlet (Olsen and Tullis 2013, Wang et al. 2018).

A culvert is a covered channel designed to pass flood waters, drainage flows, natural streams through embankment structures (Fig. 1), with a converging section at the entrance, called the inlet, a narrow section called the barrel, and a diverging section at the exit, called the outlet. The culvert channel is typically narrower than the natural river channel. The narrowest part of the culvert, i.e. the barrel, is the site of high water velocities, too often a major obstacle for small-bodied weak-swimming fish species. Sometimes, rectangular cells are placed side-by-side to increase the discharge capacity, i.e. a multicell box culvert (Fig. 1). During culvert operation, the fluid flow motion is complicated because of the boundary conditions and flow turbulence. For discharges up to the design discharge, the culvert structure operates typically as a free-surface flow. Traditionally, open channel flows have been modelled based upon one-dimensional depth-averaged equations, which predict the mean flow properties, i.e. the bulk velocity V_{mean} and water depth d , with a fair level of empiricism (Morvan et al. 2008). In relation to upstream fish passage, by far a most pertinent flow property is the velocity distribution in the vicinity of solid boundaries, given that small fish predominantly swim

upstream next to the corners and walls (Blank 2008, Katopodis and Gervais 2016, Wang et al. 2016, Cabonce et al. 2018,2019). A complete characterisation of the velocity field requires a detailed investigation which may be undertaken physically in laboratory and numerically using computational fluid dynamics (CFD).

Hybrid modelling of box culvert barrels was performed to assist the development of new guidelines for fish-friendly multi-cell box culvert designs, with a focus on the upstream passage of small-body-mass fish. The guidelines are based upon three basic concepts: (A) a smooth box culvert design without appurtenance, (B) the culvert design is optimised for fish passage for small to medium water discharges, and for flood capacity at larger discharges, and (C) low-velocity zones are provided along the wetted perimeter in the culvert barrel, and quantified in terms of a fraction of the wetted flow area where the local longitudinal velocity is less than a characteristic fish speed linked to swimming performances of targeted fish species. The approach relies upon an accurate physically-based knowledge of the entire velocity field in the barrel, specifically the longitudinal velocity map, since a number of fish behaviour observations showed that small-bodied fish swim in low-velocity zone (LVZ) boundaries. In the current study, the targeted fish species are small-bodied (less than 100 mm long) fish species and juveniles of larger fish species, although the approach and methodology are general and applicable to other fish guilds.



Figure 1. Outlet of multicell box culvert along Witton Creek (Indooroopilly QLD, Australia) on 18 March 2019 after a 40-mm rainfall storm. Looking upstream.

2 CULVERT MODELLING

2.1 Physical modelling

The physical investigation was conducted at the University of Queensland in two facilities (Fig. 2). A complete box culvert model was located in a 1 m wide flume (Fig. 2a). The box culvert barrel was 0.50 m long, 0.150 m wide and 0.105 m high. Figure 2b shows the culvert barrel flume which was 12 m long and 0.50 m wide (Fig. 2b), typical of a full-scale single-cell box culvert structure beneath a two-lane road in eastern Australia, or a 1:4 scale model of a single cell for the medium-size culvert structure seen in Figure 1. The bed and sidewalls of the flume were made of PVC and glass respectively. Upstream of the flume, the water was supplied by a 2.0 m long 1.25 m wide intake structure, fed by a constant head tank, and equipped with baffles, flow straighteners and a three-dimensional convergent leading to the 12 m long flume. The intake structure design allowed smooth inflow conditions at the flume's upstream end. At the downstream end, the flume ended with a free overfall.

The water discharges were measured with sharp-edge orifice meters designed based upon British Standards and calibrated in-situ, with an accuracy of 2%. The water depths were recorded with pointer gauges within ± 0.0005 m. The water velocities were measured with Prandtl-Pitot tube and acoustic Doppler

velocimetry, while the boundary shear stress was measured with a carefully-calibrated Preston tube (Cabonce et al. 2019).

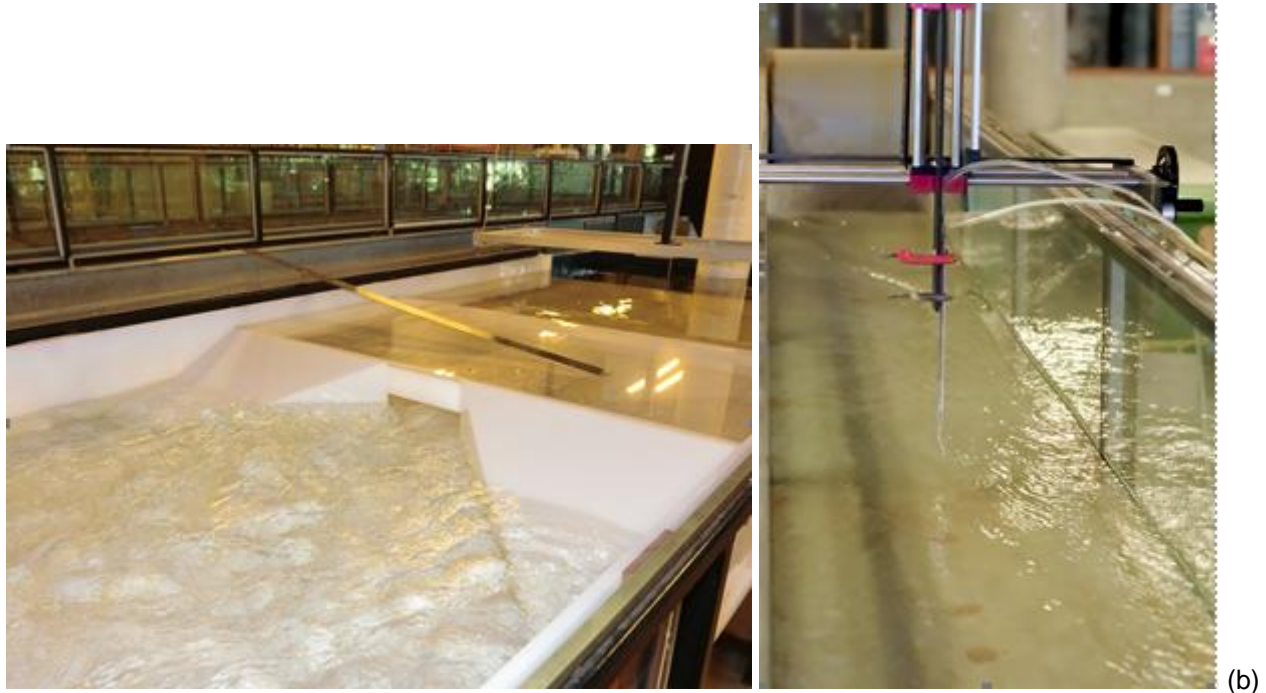


Figure 2. Physical models. (a) full culvert model ($Q = 0.012 \text{ m}^3/\text{s}$, $d_{tw} = 0.092 \text{ m}$); (b) 12 m long 0.5 m wide culvert barrel model ($Q = 0.0556 \text{ m}^3/\text{s}$) looking downstream

2.2 Numerical CFD modelling

The computational fluid dynamics (CFD) modelling was conducted with Ansys™ Fluent v. 18.0, on a Dell™ Precision T5810 workstation (Xeon® E5-1680v4 processor, 128 Gb RAM). Computational fluid dynamics modelling solves the Navier-Stokes equations of fluid motion using numerical methods. The Navier-Stokes equations describe the motion of viscous fluid, coupled with the equations of conservation of mass. A standard $k-\epsilon$ model was used to solve the flow turbulence (Rodi 1995). For smooth turbulent flows through simplistic geometries, the flow physics is mostly dominated by boundary shear on the bottom and sidewall boundaries. A simplistic turbulence model such as a $k-\epsilon$ model is sufficient to resolve the velocity field, with a relatively low computational cost (Oberkampf et al. 2004, Rodi 2017). The $k-\epsilon$ model simplifies the equation of conservation of mass and Navier-Stokes equations as:

$$\frac{\partial \rho}{\partial t} + \frac{\partial}{\partial x_j} (\rho u_j) = 0 \quad [1]$$

$$\frac{\partial \rho u_i}{\partial t} + \frac{\partial}{\partial x_j} (\rho u_i u_j) = -\frac{\partial p'}{\partial x_i} + \frac{\partial}{\partial x_j} \left[\mu_{\text{eff}} \left(\frac{\partial u_j}{\partial x_i} + \frac{\partial u_i}{\partial x_j} \right) \right] + S_M \quad [2]$$

where S_M is the sum of body forces, μ_{eff} is the effective viscosity representing flow turbulence: $\mu_{\text{eff}} = \mu + \mu_t$, μ is the fluid viscosity, μ_t is the eddy (turbulent) viscosity, p' is the modified pressure, the subscriptions i and j represent properties in the i and j directions. The standard $k-\epsilon$ model used two transport equations to describe the turbulent viscosity, in terms of the turbulent kinetic energy k and dissipation ϵ respectively (Lauder and Spalding 1974):

$$\frac{\partial}{\partial t} (\rho k) + \frac{\partial}{\partial x_i} (\rho k u_i) = \frac{\partial}{\partial x_j} \left[\left(\mu + \frac{\mu_t}{\sigma_k} \right) \frac{\partial k}{\partial x_j} \right] + G_k + G_b - \rho \epsilon - Y_M + S_K \quad [3]$$

$$\frac{\partial}{\partial t} (\rho \epsilon) + \frac{\partial}{\partial x_i} (\rho \epsilon u_i) = \frac{\partial}{\partial x_j} \left[\left(\mu + \frac{\mu_t}{\sigma_\epsilon} \right) \frac{\partial \epsilon}{\partial x_j} \right] + C_{1\epsilon} \frac{\epsilon}{k} (G_k + C_{3\epsilon} G_b) - C_{2\epsilon} \rho \frac{\epsilon^2}{k} + S_\epsilon \quad [4]$$

where G_k represents the generation of turbulent kinetic energy due to the mean velocity gradient, G_b is the generation of turbulent kinetic energy due to buoyancy, Y_M represents the contribution of the fluctuating dilatation in compressible turbulence to the overall dissipation rate. $C_{1\varepsilon}$, $C_{2\varepsilon}$ and $C_{3\varepsilon}$ are constants, σ_k and σ_ε are the turbulent Prandtl numbers for k and ε respectively, S_k and S_ε are user-defined source terms. The turbulent viscosity μ_t is computed by combining k and ε as: $\mu_t = \rho C_\mu k^2/\varepsilon$. By default, ANSYS Fluent used the following values: $C_{1\varepsilon} = 1.44$, $C_{2\varepsilon} = 1.92$, $C_\mu = 0.09$, $\sigma_k = 1.0$, $\sigma_\varepsilon = 1.3$.

The two-phase flow interface in the culvert barrel was tracked by a volume of fluid (VOF) method (Hirt and Nichols 1981). In VOF, a colour function C was introduced, defined as 0 in one phase and 1 in the other. Herein, the primary phase was selected to be air (the lighter medium) and secondary phase water. The fluid density and viscosity were calculated based on respective fractions of local colour function. Finally the near-wall areas of the flow were treated by a built-in standard wall function in ANSYS Fluent. The wall function was based on the work of Launder and Spalding (1974), widely used in industrial flows.

The numerical domain represented a single box culvert barrel (Fig. 3). The barrel length was $L = 12$ m. The width and height of the numerical domain were prescribed according to the internal width and height of the culvert barrel, B_{cell} and D_{cell} respectively, with $0.5 \text{ m} < B_{\text{cell}} < 2.4 \text{ m}$ and $1 < (B_{\text{cell}}/D_{\text{cell}}) < 2$. The inlet plane, marked in yellow and blue in Figure 3, was split into two velocity inlets, one for water (yellow) and one for air (blue). The outlet plane (green) was a single outlet for both phases, and set to be a pressure outlet. A free-surface level was required to set up the outlet for open channel flow, and this outlet depth d_{out} was prescribed according to the tailwater level for the test case. In general, $d_{\text{out}} \approx d_{\text{tw}}$, where d_{tw} is the tailwater depth in the downstream floodplain.

The numerical CFD modelling was conducted in two successive stages: (1) transient flow simulation in a 3D culvert channel with coarse mesh; the coarse mesh consisted of uniform squares with 0.05-0.1 m grid size throughout the numerical domain; and (2) transient flow simulation in a 3D culvert channel with refined mesh; the mesh was refined into non-uniform gradually varied squares using a bias function (Leng and Chanson 2018). Biased mesh with refinement near the walls and sidewalls were essential to simulate realistic flow patterns near the boundaries. A bias factor of 20-30 was used typically for all cases, resulting in a growth factor $r = 1.1$ -1.2. After refinement, the smallest grid size in the vertical y and transverse z directions was between 0.001 m to 0.005 m depending on the size of the culvert barrel. All CFD models were solved using a k - ε turbulence model. The transient formulation was solved implicitly in first order, with a second order upwind scheme for momentum, first order upwind scheme for turbulent kinetic energy and turbulent dissipation rate. The convergence was ensured by reducing residuals of all parameters to 10^{-4} or less. All simulations were run for a physical time span of over 60 s to ensure a steady equilibrium flow and the conservation of mass was achieved between inlet and outlet. The computation time for a complete run was approximately 12-24 hours on a HPC workstation.

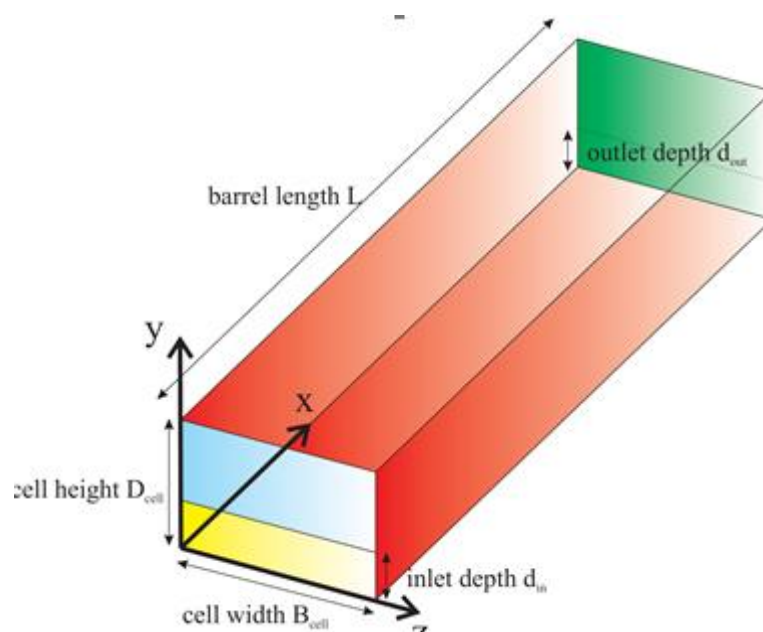


Figure 3. Three-dimensional (3D) definition sketch of numerical domain with colour-coded boundaries: Blue = air inlet (velocity inlet); Yellow = water inlet (velocity inlet); Red = walls (wall condition); Green = outlet for air & water (pressure outlet).

3 NUMERICAL RESULTS AND VALIDATION

A systematic comparison between physical and numerical data was conducted with smooth rectangular culvert barrel channel (roughness height $k_s \approx 10^{-4}$ m). Typical results are presented in Figure 4, with Q the water discharge, x the longitudinal coordinate along the culvert barrel positive downstream and S_o the barrel invert slope. Figure 4a shows the comparison in terms of free-surface elevations. The results demonstrated a good agreement between the 1D calculations, CFD results and experimental data in terms of free-surface elevation throughout the culvert channel. A key issue was to use a realistic outlet depth d_{out} . The CFD model used a pressure outlet, which was very sensitive to the prescribed downstream free-surface level at the outlet. Herein, experimentally measured values were used at the outlet boundary to prescribe the tailwater depth, which was considered very important in reproducing the correct free-surface profile.

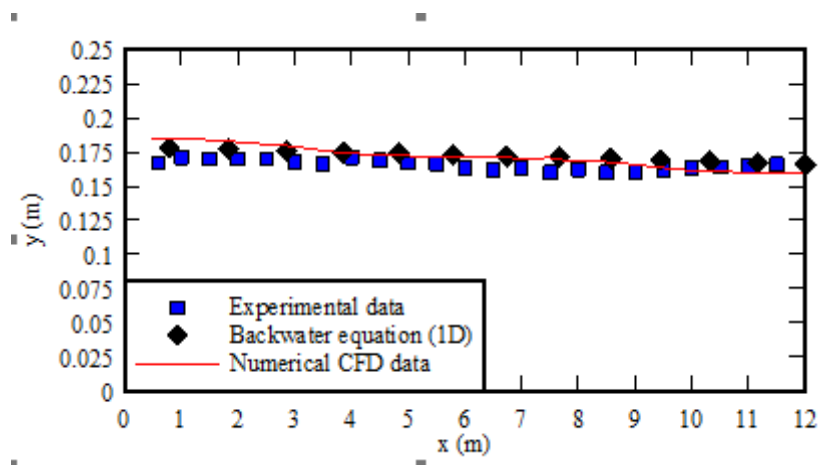


Figure 4. Free-surface profile for $Q = 0.0556$ m³/s, $B_{cell} = 0.5$ m, $S_o = 0$. Comparison between physical measurements (Cabonce et al. 2017), 1D theoretical calculations (backwater equation) and numerical CFD modelling

The cross-section velocity contour for longitudinal velocity can be calculated using the CFD model. Typical result at $x = 8$ m, i.e. 8 m downstream of the inlet is shown in Figure 5a. The data showed good agreement with experimental findings by Cabince et al. (2017). Detailed comparison of vertical profile and boundary layer development was performed for locations near the side walls (0.02 m, 0.04 m and 0.08 m from the sidewalls). Results are presented in Figure 5b. Overall, the CFD data compared favourably to physical results for all transverse locations near walls, where low velocity zones are likely to occur. The model showed better estimation at locations slightly away from the side wall ($z = 0.08$ m), highlighting some limitation in standard $k-\epsilon$ model. It was also found that the standard $k-\epsilon$ model has a tendency of over-estimating longitudinal velocities at locations outside of the sidewall boundary layer. On the channel, centerline, the free-stream velocity was found to be 5-10% higher than the physical observations (Leng and Chanson 2018, Chanson and Leng 2019).

Overall, the results showed the capacity of a CFD model to predict the three-dimensional flow field in a smooth culvert barrel, which could be used to estimate accurately low-velocity zones (LVZs) and to design a fish-friendly box culverts. The systematic validation against physical data is uppermost critical to ascertain the performances of a numerical model, and can be sensitive to a range of inflow conditions, boundary parameters, and the grid mesh quality and size (Leng and Chanson 2018, Zhang and Chanson 2018).

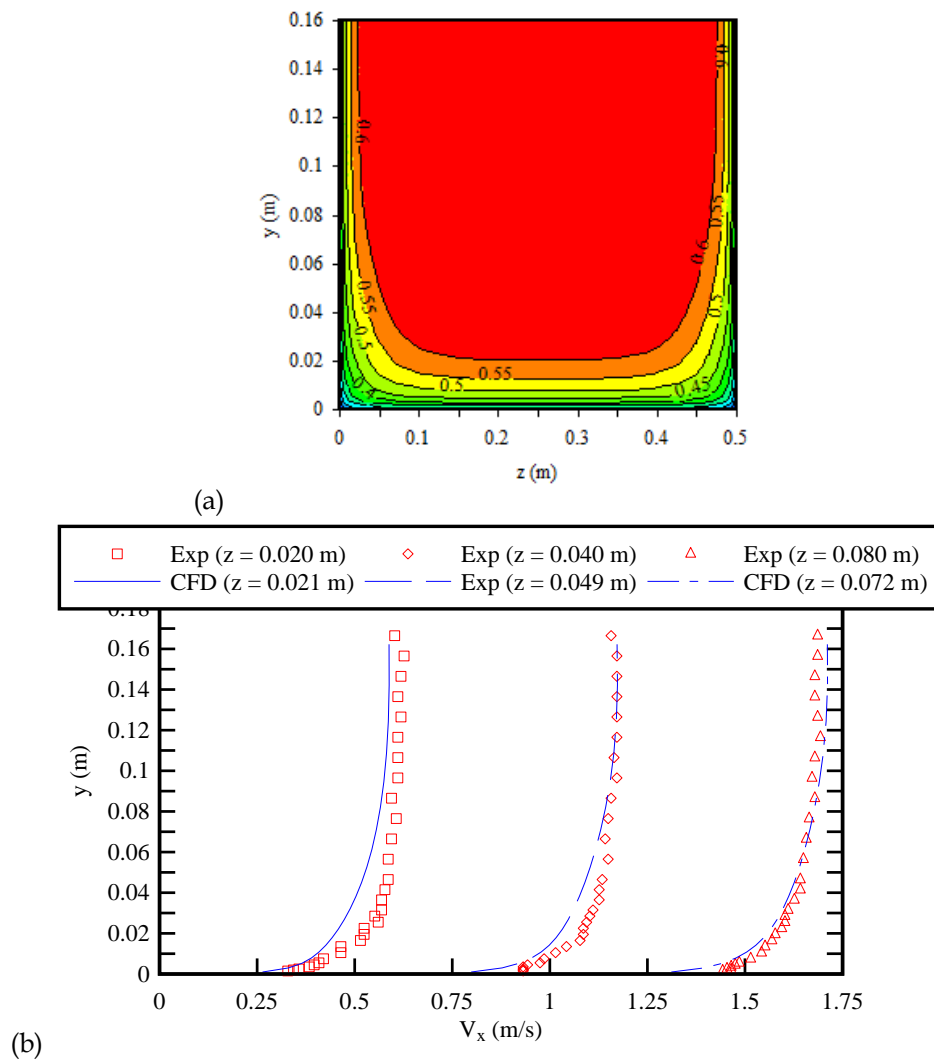


Figure 5. Box culvert barrel flow at less-than-design flow conditions for $Q = 0.0556 \text{ m}^3/\text{s}$, $B_{\text{cell}} = 0.5 \text{ m}$, $S_o = 0$. Comparison between physical measurements (Cabonce et al. 2017) and numerical CFD modelling (a) velocity contour at $x = 8 \text{ m}$; (b) longitudinal velocity V_x distribution near wall (horsizontal axis offset by +0.5 and +1 for locations further from wall).

In terms of fish passage in standard box culverts, recent field observations and large-size laboratory studies showed that the fish swim preferentially close to sidewalls particularly in the corners, in regions of low velocity and high turbulence intensity (Blank 2008, Goettel et al. 2015, Wang et al. 2016, Cabonce et al. 2018,2019). The observations highlighted the "sweet spots" that the fish exploit, i.e. regions of slower-velocity and high-turbulence. The finding was consistent with energetic considerations since the rate of mechanical work exerted by a fish is equal to the thrust times the relative fish speed, hence proportional to the cube of the local fluid velocity (Wang and Chanson 2018a,b). These "sweet spots" were basically low-velocity-zones along the wetted perimeter. In turn, the accurate estimate for the low velocity zone dimensions is critical to upstream fish passage. The calculations must be generalised, with self-defined criteria for low velocity, independently of the hydrology requirement. The current study examined the relationship between local velocity V_x and the associated flow area where the local velocity is less than that velocity (Chanson and Leng 2019). Both numerical and experimental data are summarised in dimensionless form in Figure 6. Overall, the CFD cases showed a same monotonic trend (Fig. 6), with quantitatively close results. The results seemed to show little effects to the aspect ratio B_{cell}/d and Reynolds number. Figure 6 presents also a comparison between present CFD and experimental works. In Figure 6, all the data are further compared to an analytical solution for the equation of conservation of mass for a two dimensional turbulent flow, assuming a $1/N$ -th velocity distribution power law:

[5]

$$A = \left(\frac{N}{N+1} \right)^N \times \left(\frac{V_x}{V_{\text{mean}}} \right)^N$$

with A the percentage of flow area between 0 and 1. Equation (5) is plotted for $N = 4.5$ in Figure 6, and compared to physical and CFD data, as well as to a best-fit trendline of experimental data. The experimental data showed overall a larger area fraction for the same relative velocity compared to the CFD data. An average between the two curves could be considered to use in practice in predicting the relationship between flow area associated with low-velocity zones, although Equation (5) for $N = 4.5$ may be conservative estimated of the low-velocity zone area.

It is worthwhile to highlight the advantages of the dimensionless presentation of Figure 6 to quantify the size of low-velocity zones to facilitate upstream fish passage. First the plot is independent of hydrological implication and design flood event, which could vary upon requirement of different councils and sites. Second the results are independent of the barrel culvert cell size and downstream tailwater conditions.

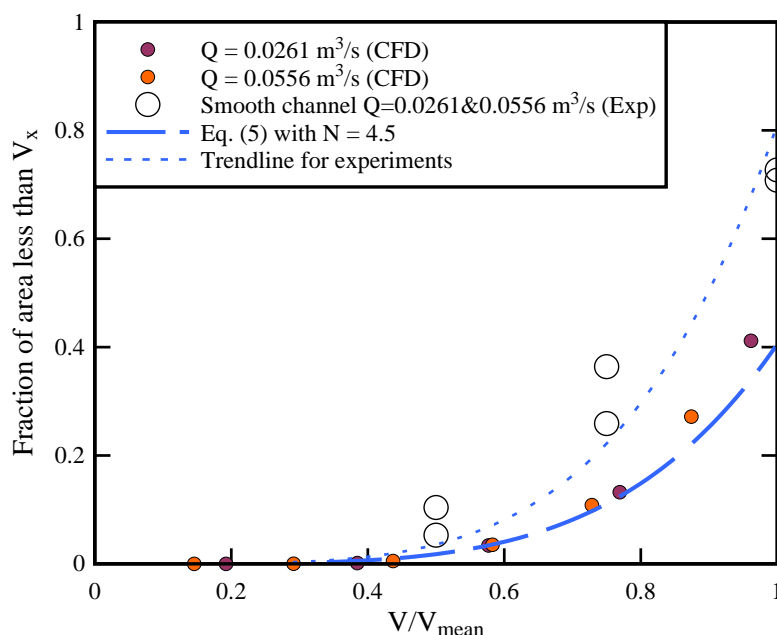


Figure 6. Dimensionless area fraction of flow less than a relative longitudinal velocity V_x/V_{mean} , where V_{mean} is the bulk velocity i.e. cross-sectional mean velocity in the barrel. Present numerical data compared to past experimental studies (Cabonce et al. 2017), Equation (5) assuming $N = 4.5$ (blue long dash line) and best fit trendline for physical experiments (blue dotted line). All data obtained for $3 < B_{\text{cell}}/d < 5$.

4 APPLICATION TO HYDRAULIC DESIGN GUIDELINES FOR SMALL-BODY-MASS FISH PASSAGE

4.1 Presentation

With current hydraulic engineering design practices, the optimum size of a culvert is the smallest barrel size allowing for inlet control operation (Herr and Bossy 1965, Chanson 2004). Such an approach is focused on design flow conditions solely and rarely considers less-than-design flow conditions ($Q < Q_{\text{des}}$), although fish passage may occur as soon as the water discharge is non-zero ($Q > 0$). New design guidelines for fish-friendly box culverts are needed and a practical challenge is matching biological data, e.g. swimming performances, to engineering requirements and hydrodynamic measurements, because of a lack of standardisation in swim tests (Kemp 2012, Katopodis and Gervais 2016, Wang and Chanson 2018b). In the current study, new hydraulic engineering design guidelines for fish-friendly box culverts are developed based upon three basic concepts:

(A) the culvert barrel walls are smooth and upstream fish passage is provided without any other form of boundary treatment and appurtenance;

(B) the culvert design is optimised for fish passage for water discharges $Q < Q_T$; and it is optimised in terms of flood capacity for $Q_T < Q < Q_{\text{des}}$, with Q_T an upper threshold of less-than-design discharge; and

(C) since fish predominantly swim upstream next to the channel corners and sidewalls, including small-bodied Australian native fish species, the swimming performance data are related to a fraction (i.e. percentage) of the wetted flow area where: $0 < V_x < U_{\text{fish}}$ (Chanson and Leng 2018,2019), with V_x the local time-averaged longitudinal velocity component and U_{fish} a characteristic swimming speed of targeted fish species; a truly novel aspect of this approach is the provision of a minimum relative flow area where the longitudinal water velocity is less than a characteristic fish swimming speed.

One may contrast past and novel design guidelines of fish-friendly culverts. Previously, fish-friendly culvert design guidelines were based upon some bulk velocity criterion, i.e. a maximum bulk velocity largely attributed to the culvert across the full flow range, neither of which appear to be relevant to reality. In contrast, the new design guidelines take into account that fish swim predominantly along the sidewalls, and that, at higher discharges, fish passage is generally not possible given the constraints of the culvert design relative to the physical capabilities of small-bodied fish.

4.2 Application

For practical applications, the hydraulic engineering calculations are first conducted for design flow conditions. The barrel size is selected by a test-and-trial procedure, in which both inlet control and outlet control calculations are performed for design flow conditions. The optimum size is the smallest barrel size allowing for an afflux less than the maximum acceptable afflux at design discharge Q_{des} (Herr and Bossy 1965, Chanson 2004). The second part of the design corresponds to a culvert operation for less-than-design flow: i.e. $Q \leq Q_T$, for which a minimum relative flow area must experience local time-averaged velocities less than the characteristic fish swimming speed (U_{fish}). When choosing the minimum fish swimming speed for the site, in relation to the species and size classes of expected fish, the local fisheries department should be consulted.

The hydraulic calculations of a culvert operating at less-than-design flow are not trivial (Chanson and Leng 2019). For a mild flood plain slope, the culvert operates with outlet control for $Q < Q_{\text{des}}$. The flow in the entire culvert system is subcritical and the calculations are best started from the downstream end, i.e. the tailwater conditions. The complete calculations involve (a) the estimate of the form losses in the culvert outlet and transition to the downstream flood plain, (b) the hydrodynamic calculations of the culvert barrel flow and the boundary friction, and (c) the application of the Bernoulli principle to the flow convergence in the transition from the upstream flood plain to the inlet and in the culvert inlet. For a culvert in a steep catchment, the same type of hydrodynamic calculations is conducted, albeit starting from the upstream end, i.e. the headwater conditions.

When fish passage is a requirement for $Q < Q_T$, a number of basic assumptions may be considered to simplify the hydraulic engineering calculations at less-than design discharges: [1] the flood plain's longitudinal slope is mild and the flood plain operates with subcritical flow conditions for $Q < Q_T$; [2] the free-surface elevation in the barrel equals the tailwater free-surface elevation; in first approximation, the water depth d_{barrel} in the barrel is equal to the tailwater depth d_{tw} ; and [3] there is a monotonic relationship between the relative low velocity zone (LVZ) area where the dimensionless velocity V_x/V_{mean} is less than $U_{\text{fish}}/V_{\text{mean}}$, and the dimensionless targeted fish swimming speed $U_{\text{fish}}/V_{\text{mean}}$; Figure 6 and Equation (5) may be used to quantify the relative size of the LVZ area.

Practically, the most stringent hydrodynamic conditions for upstream passage of small-bodied fish take place for $Q = Q_T$. In turn the hydraulic calculations for upstream fish passage are typically focused on $Q = Q_T$. Chanson and Leng (2019) developed complete applications.

5 CONCLUSIONS

Road crossings and culverts are known to block the upstream passage of fish, particularly for small-body-mass fish species and juveniles of large body fish. Using a combination of physical and numerical CFD modelling, novel guidelines were developed for smooth box culverts without appurtenance, with a novel approach based upon the basic concepts: (I) the culvert design is optimised for fish passage for small to medium water discharges, and for flood capacity for larger discharges, and (II) low-velocity zones are provided along the wetted perimeter in the culvert barrel, and quantified in terms of a fraction of the wetted flow area where the local longitudinal velocity is less than a characteristic fish speed linked to swimming performances of targeted fish species. The approach relies upon an accurate physically-based knowledge of the entire velocity field in the culvert barrel, especially next to the fixed boundaries, given that behavioural observations confirmed showed that fish prefer to swim upstream in low-velocity zones (LVZs) next to the sidewalls and bottom corners.

The present approach develops a physically-based rationale for fish-friendly standard box culvert design, embedding state-of-the-art hydrodynamic calculations into current hydraulic engineering design methods to yield cost-effective outcomes. While the focus of the guidelines is on the upstream passage of small-body-mass fish, typical of Australian native fish species, the approach and methodology are relevant to many more fish species for which the excessive box culvert barrel velocities hinder their upstream passage. The method is more general than previous attempts, yet simple and cost effective enough to be widely endorsed by the various stakeholders. By bridging the gap between engineering and biology, this novel approach may contribute to the restoration of catchment connectivity for small-body-mass fish. Finally, it must be stressed that the design of a culvert that is intended to be constructed would require the certification of a professional civil engineer.

ACKNOWLEDGEMENTS

The authors thank Dr Matt Gordos (NSW DPI Fisheries, Australia), Marcus Riches (NSW DPI Fisheries) and Professor Colin Apelt (The University of Queensland, Australia) for helpful discussions and inputs. The authors acknowledge the assistance of Ms Matilda Meppem and Mr Tianwei Yin (The University of Queensland, Australia) in conducting a number of tests using CFD models. The financial support through the Australian Research Council (Grant LP140100225) is acknowledged.

Hubert Chanson has competing interest and conflict of interest with Craig E. Franklin.

REFERENCES

- Anderson, G.B., Freeman, M.C., Freeman, B.J., Straight, C.A., Hagler, M.M., and Peterson, J.T. (2012). Dealing With Uncertainty When Assessing Fish Passage Through Culvert Road Crossings. *Environmental Management*, Vol. 50, pp. 462-477.
- Blank, M.D. (2008). Advanced Studies of Fish Passage through Culverts: 1-D and 3-D Hydraulic Modelling of Velocity, Fish Energy Expenditure, and a New Barrier Assessment Method. *Ph.D. thesis*, Montana State University, Department of Civil Engineering, 231 pages.
- Briggs, A.S., and Galarowicz, T.L. (2013). Fish Passage through Culverts in Central Michigan Warmwater Streams. *North American Journal of Fisheries Management*, Vol. 33, pp. 652-664.
- Cabonce, J., Fernando, R., Wang, H., and Chanson, H. (2017). Using Triangular Baffles to Facilitate Upstream Fish Passage in Box Culverts: Physical Modelling. *Hydraulic Model Report No. CH107/17*, School of Civil Engineering, The University of Queensland, Brisbane, Australia, 130 pages (ISBN 978-1-74272-186-6).
- Cabonce, J., Wang, H., and Chanson, H. (2018). Ventilated Corner Baffles to Assist Upstream Passage of Small-Bodied Fish in Box Culverts. *Journal of Irrigation and Drainage Engineering*, ASCE, Vol. 144, No. 8, Paper 0418020, 8 pages (DOI: 10.1061/(ASCE)IR.1943-4774.0001329).
- Cabonce, J., Fernando, R., Wang, H., and Chanson, H. (2019). Using Small Triangular Baffles to Facilitate Upstream Fish Passage in Standard Box Culverts. *Environmental Fluid Mechanics*, Vol. 19, No. 1, pp. 157-179 (DOI: 10.1007/s10652-018-9604-x).
- Chanson, H. (2004). *The Hydraulics of Open Channel Flow: An Introduction*. Butterworth-Heinemann, 2nd edition, Oxford, UK, 630 pages (ISBN 978 0 7506 5978 9).
- Chanson, H., and Leng, X. (2018). On the Development of Hydraulic Engineering Guidelines for Fish-Friendly Standard Box Culverts, with a Focus on Small-Body Fish. *Civil Engineering Research Bulletin No. 25*, School of Civil Engineering, The University of Queensland, Brisbane, Australia, 79 pages.
- Chanson, H., and Leng, X. (2019). There is Something Fishy about Turbulence - Why Novel Hydraulic Engineering Guidelines can assist the Upstream Passage of Small-Bodied Fish Species in Standard Box Culverts. *Civil Engineering Research Bulletin No. 26*, School of Civil Engineering, The University of Queensland, Brisbane, Australia (ISBN 978-1-74272-234-4).
- Goettel, M.T., Atkinson, J.F., and Bennett, S.J. (2015). Behavior of western blacknose dace in a turbulence modified flow field. *Ecological Engineering*, Vol. 74, pp. 230-240.
- Herr, L. A., and Bossy, H.G. (1965). Capacity Charts for the Hydraulic Design of Highway Culverts. *Hydraulic Eng. Circular*, US Dept. of Transportation, Federal Highway Admin., HEC No. 10, March.
- Hirt, C., and Nichols, B. (1981). Volume of Fluid (VOF) method for the dynamics of free boundaries. *Journal of Computational Physics*, Vol. 39, No. 1, pp. 201-225.
- Katopodis, C., and Gervais, R. (2016). Fish Swimming Performance Database and Analyses. *DFO CSAS Research Document No. 2016/002*, Canadian Science Advisory Secretariat, Fisheries and Oceans Canada, Ottawa, Canada, 550 pages.
- Kemp, P. (2012). Bridging the Gap between Fish Behaviour, Performance and Hydrodynamics: an Ecohydraulics Approach to Fish Passage Research. *River Research and Applications*, Vol. 28, pp. 403-406 (DOI: 10.1002/rra.1599).

- Lauder, B.E., and Spalding, D.B. (1974). The numerical computation of turbulent flows. *Computer Methods in Applied Mechanics and Engineering*, Vol. 3, No. 2, pp. 269-289.
- Leng, X., and Chanson, H. (2018). Modelling Low Velocity Zones in Box Culverts to Assist Fish Passage. *Proceedings of 21st Australasian Fluid Mechanics Conference*, Adelaide, Australia, 10-13 December, Editors T.C.W. Lau and R. M. Kelso, Paper 547, 4 pages.
- Lintermans, M. (2013). Recovering Threatened Freshwater Fish in Australia. *Marine and Freshwater Research*, Vol. 64, pp. iii-vi (DOI: 10.1071/MFv64n9_IN).
- Macintosh, J.C. (1990). Hydraulic characteristics in channels of complex cross-section. *Ph.D. thesis*, School of Civil Engineering, The University of Queensland, Brisbane, Australia, 505 pages.
- Morvan, H., Knight, D., Wright, N., Tang, X., and Crossley, A. (2008). The Concept of Roughness in Fluvial Hydraulics and its Formulation in 1D, 2D and 3D Numerical Simulation Models. *Journal of Hydraulic Research*, Vol. 46, No. 2, pp. 191-208.
- Naot, D. and Rodi, W. (1982). Numerical simulations of secondary currents in channel flow. *Journal of Hydraulic Division*, ASCE, Vol. 108, No. HY8, pp. 948–968.
- Nezu, I. and Rodi, W. (1985). Experimental study on secondary currents in open channel flow. *Proceedings of the 21st IAHR Congress*, IAHR, Melbourne, pp. 115-119.
- Nikuradse, J. (1926). Turbulente Stromung im Innem des rechteckigen offenen Kanals. *Forschungsarbeiten, Heft 281*, pp. 36-44 (in German).
- Oberkampf, W.L., Trucano, T.G., and Hirsch, C. (2004). Verification, validation, and predictive capability in computational engineering and physics, *Applied Mechanics Review*, ASME, Vol. 57, No. 5, pp. 345-384.
- Olsen, A. and Tullis, B. (2013). Laboratory Study of Fish Passage and Discharge Capacity in Slip-Lined, Baffled Culverts. *Journal of Hydraulic Engineering*, ASCE, Vol. 139, No. 4, pp. 424–432
- Rodi, W. (1995). Impact of Reynolds-Average Modelling in Hydraulics. *Proceedings Mathematical and Physical Sciences*, Vol. 451, No. 1941, pp. 141-164.
- Rodi, W. (2017). Turbulence Modeling and Simulation in Hydraulics: A Historical Review. *Journal of Hydraulic Engineering*, ASCE, Vol. 143, No. 5, Paper 03117001, 20 pages (DOI: 10.1061/(ASCE)HY.1943-7900.0001288).
- Wang, H., Chanson, H., Kern, P., and Franklin, C. (2016a). Culvert Hydrodynamics to enhance Upstream Fish Passage: Fish Response to Turbulence. *Proceedings of 20th Australasian Fluid Mechanics Conference*, Australasian Fluid Mechanics Society, G. Ivey, T. Zhou, N. Jones, S. Draper Editors, Perth WA, Australia, 5-8 December, Paper 682, 4 pages.
- Wang, H., and Chanson, H. (2018a). Modelling Upstream Fish Passage in Standard Box Culverts: Interplay between Turbulence, Fish Kinematics, and Energetics. *River Research and Applications*, Vol. 34, No. 3, pp.244-252 (DOI: 10.1002/rra.3245).
- Wang, H., and Chanson, H. (2018b). On Upstream Fish Passage in Standard Box Culverts: Interactions between Fish and Turbulence. *Journal of Ecohydraulics*, IAHR, Vol. 3, No. 1, pp. 18-29 (DOI: 10.1080/24705357.2018.1440183).
- Wang, H., Uys, W., and Chanson, H. (2018). Alternative Mitigation Measures for Fish Passage in Standard Box Culverts: Physical Modelling. *Journal of Hydro-environment Research*, IAHR, Vol. 19, pp. 214-223 (DOI: 10.1016/j.jher.2017.03.001).
- Xie, Q. (1998). Turbulent Flows in Non-Uniform Open Channels: Experimental Measurements and Numerical Modelling. *Ph.D. thesis*, School of Civil Engineering, The University of Queensland, Brisbane, Australia, 358 pages.
- Zhang, G., and Chanson, H. (2018). Three-Dimensional Numerical Simulations of Smooth, Asymmetrically Roughened, and Baffled Culverts for Upstream Passage of Small-bodied Fish. *River Research and Applications*, Vol. 34, No. 8, pp. 957-964 (DOI: 10.1002/rra.3346).

Youtube video movie

Fish-friendly waterways and culverts - Integration of hydrodynamics and fish turbulence interplay & interaction
{<https://youtu.be/GGWTWDOmoSQ>}